European Commission

JRC TECHNICAL REPORTS

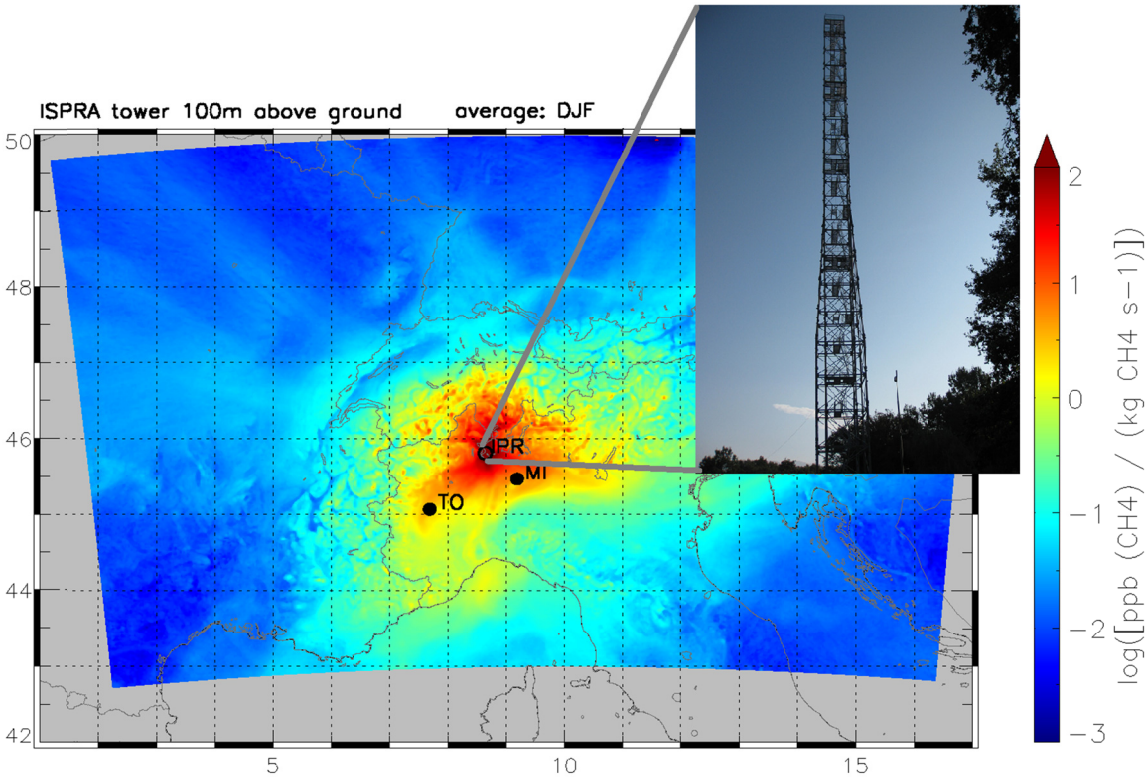

Analysis of the sensitivity of atmospheric measurements at the JRC Ispra Atmosphere - Biosphere - Climate Integrated monitoring Station

Footprint analysis based on FLEXPART-COSMO model

Peter Bergamaschi and Dominik Brunner[1]

2015

Report EUR 27131 EN

Joint Research Centre

European Commission
Institute for Environment and Sustainability

Contact information
Peter Bergamaschi
Joint Research Centre, Institute for Environment and Sustainability
Air and Climate Unit (H02), TP 123
I-21027 Ispra (Va), Italy
E-mail: peter.bergamaschi@jrc.ec.europa.eu
Tel.: +39 0332 789621

[1]Dominik Brunner
Swiss Federal Laboratories for Materials Science and Technology (EMPA)
Überlandstrasse 129
CH-8600 Dübendorf, Switzerland
E-mail: dominik.brunner@empa.ch

JRC Science Hub
https://ec.europa.eu/jrc

JRC94909

EUR 27131 EN

ISBN 978-92-79-46164-4 (PDF)

ISSN 1831-9424 (online)

doi: 10.2788/234440

Luxembourg: Publications Office of the European Union, 2015

Abstract

The sensitivity of atmospheric concentration measurements at the JRC Ispra Atmosphere - Biosphere - Climate Integrated monitoring Station to emissions on different spatial scales ('source-receptor relationship') is analysed using the Lagrangian particle dispersion model FLEXPART, driven by meteorological fields from the nested COSMO-2 / COSMO-7 numerical weather prediction system at a horizontal resolution of 2 km / 7 km, respectively. The sensitivity of the atmospheric signal shows significant variations on diurnal, synoptic and seasonal scales. During night, the sensitivity is usually dominated by the area 40-60 km around the station, while daytime footprints are much larger, typically dominated by the area at distances of more than 60 km. During summer daytime, the radius τ_{s50} (at which the cumulative surface sensitivity reaches 50% of the total sensitivity) is about 187 km on average. Furthermore, a clear diurnal cycle in local wind direction is visible due to a regional mountain - lake/valley wind system, leading to a significant diurnal cycle of the sensitivity (north-west vs. south-east), especially during summer time.
Our analysis shows that the future sampling at the Ispra tall tower 100m above ground significantly reduces the impact of local emissions (~3-10 km around the station) compared to the previously used sampling height of 15m above ground.

Table of Contents

1. Introduction

Atmospheric measurements combined with inverse modelling can inform on emissions on different spatial scales (e.g. [*Bergamaschi et al.*, 2015]). At the monitoring station Ispra on the premises of the Joint Research Centre site, greenhouse (GHG) measurements started end 2007, sampling air at an altitude of 15m above ground [*Putaud et al.*, 2014; *Scheeren and Bergamaschi*, 2011]. In 2014, a 100m tall tower has been setup and the construction of a new station building has been started, which will be completed and equipped with instrumentation in 2015.

The new 'Atmosphere - Biosphere - Climate Integrated monitoring Station' (ABC-IS) will integrate the JRC GHG measurements, the EMEP-GAW (European Monitoring and Evaluation Programme - Global Atmospheric Watch) air quality station, and further measurements of various atmospheric constituents and parameters [*Putaud et al.*, 2014].

For interpretation of the atmospheric measurements, knowledge of the origin of sampled air masses is essential. In this study we present a detailed analysis of the sensitivity of the atmospheric concentrations to emissions on different spatial scales. The sensitivity is defined throughout this report as the 'source-receptor relationship', describing the response function of atmospheric concentrations at the monitoring station to emissions [*Stohl et al.,* 2005]. The analysis is based on the calculation of 3-dimensional back trajectories, using the Lagrangian particle dispersion model FLEXPART, driven by meteorological fields from the nested COSMO-2 / COSMO-7 numerical weather prediction modelling system at horizontal resolutions of 2 km / 7 km, respectively. The model's representation of the local meteorology is evaluated against measurements at the ARPA and EMEP meteo stations near the two masts.

The analysis is performed for 2011, investigating the sensitivity to emissions both for the 15m sampling mast (in order to support the interpretation of the past GHG measurements) and the new 100m tall tower in order to investigate the benefit of the increased sampling height. Furthermore, the objective of the characterization of the 'footprint' at very high spatial resolution is to support the integration of the Ispra monitoring station into the 'Integrated Carbon Observation System (ICOS)' (http://www.icos-infrastructure.eu/), the new European integrated monitoring network for atmospheric GHGs.

2. COSMO / FLEXPART simulations

3-dimensional 5-day back trajectories are calculated using the Lagrangian particle dispersion model FLEXPART which considers grid-resolved advective as well as subgrid-scale turbulent and convective transport [*Stohl et al.*, 2005]. 50000 particles are released in the model at the Ispra site (45.815^{o}N, 8.636^{o}E) at both sampling heights (15m / 100m above ground) in 3-hourly time intervals. Particle transport is driven by hourly meteorological fields from the Consortium for Small-Scale Modelling (COSMO) numerical weather prediction modelling system operated by MeteoSwiss. The COSMO system is run in a nested configuration, with a horizontal resolution of 2.2 km for the inner domain (COSMO-2), covering Switzerland and significant parts of adjacent countries (including Northern Italy), and a horizontal resolution of 6.6 km for the outer domain (COSMO-7), covering large parts of Europe between about 37°N and 57°N including most of Italy (see e.g. Figures 4a and 4b). Hourly analysis fields are produced for both model domains applying the observational nudging technique [*Schraff*, 1997] to surface observations of pressure, relative humidity and wind. In the COSMO-2 configuration, convection is explicitly resolved whereas in COSMO-7 convection is

parameterized using the Tiedtke scheme [*Tiedtke*, 1987] which has also been integrated into the FLEXPART model. Please note that for model output shown in this report for the COSMO-7 grid domain, the simulations were generally based on the nested configuration, i.e. driven by COSMO-2 meteorology in the inner parts of the domain and by COSMO-7 in the outer parts.
Figure 1 shows the model topography around the Ispra station (for the 2 km resolution), demonstrating that the complex topography in this area is reasonably well resolved.

3. Meteorology

Simulated and observed meteorological parameters are shown in Figures 2a - 2d. Measurements are from the Agenzia Regionale per la Protezione dell'Ambiente della Lombardia (ARPA) meteo station relatively close to the 15m mast of the current/past GHG measurements, and in addition for wind speed and wind direction also from the JRC EMEP station (close to the location of the new 100m tower). Measurements of temperature and pressure are in general very well represented by COSMO-2, except some periods, when the diurnal cycle of the temperature is underestimated, especially during winter months. The pressure typically shows a small daily minimum coinciding with the temperature maximum in the afternoon, which is very well reproduced by the model.
Simulated wind speeds (at 10m) are in general higher than observations at both meteo stations, probably due to the limited representativeness of the measurements. Minor overpredictions of 10m wind speeds by COSMO-2, though of much smaller magnitude, have also been reported for other sites [*Oney et al.*, 2015]. While the ARPA measurements have been made on the top of a building, the EMEP measurements are made at a 10m mast. However, nearby trees probably reduce the observed wind speed at both sites, and limit the representativeness of the measurements. Usually the wind speeds measured at the ARPA station are lower than those measured at the EMEP site. In addition, the frequency distribution of wind direction ('wind roses') shows significant differences (Figure 3) between the two measurement sites despite their only relatively small spatial separation of about 1 km. Despite these differences, both measurement data sets often show a clear diurnal cycle of the wind direction, most pronounced during summer for 'clear-sky' days with pronounced diurnal cycles of the temperature. This diurnal pattern is due to a regional mountain - lake/valley wind system, leading to southerly winds during daytime, and northerly winds during night. Between February and October the monthly average diurnal cycles typically show a rotation of wind direction, starting in the morning from North (0° / 360°) anti-clockwise (i.e. over West) to South (~180°) in the afternoon. In the late afternoon / early evening the southerly flow collapses and the wind direction is reverting to North. The rotation in wind direction during day is relatively consistent between measurements and COSMO-2 simulations. The reversal of wind direction and dominance of northerly winds during night is also relatively consistent between COSMO-2 and the ARPA measurements (however only a limited number of 'valid' wind direction measurements (above the chosen threshold for the wind speed of 0.5 m/s) are available for this station), while the EMEP measurements often show south-easterly wind direction (~90°...180°) during night (clearly visible especially in August and September). These south-easterly winds during night are likely due to katabatic winds during night, downhill a slope south-east of the EMEP station. Please note that in the plot of the wind roses in Figure 3 only those hourly data records were used, for which the wind speed is above the threshold of 0.5 m/s for all three data sets; therefore this katabatic wind component is not visible in this presentation.

The dominance of southerly flow in the afternoon typically coincides with a diurnal maximum in wind speed (clearly visible between March and October), which is qualitatively consistent between COSMO-2 simulations and measurements. Future measurements of meteorological parameters on the new 100m tower will be much more representative compared to the current sites and will provide additional valuable information for more quantitative validation of the transport simulations.

4. Footprints

Figures 4a and 4b show seasonal average sensitivities of atmospheric concentration measurements to emissions ('footprints') from the FLEXPART 5-day back trajectories for winter (DJF) and summer (JJA), for the COSMO-2 and COSMO-7 domains, respectively. These sensitivities are calculated in units of (ppb CH_4) / (kg CH_4 s^{-1}), i.e. relating the emissions in the area of the model domain to the concentration signal at the Ispra monitoring station. We have chosen here CH_4 as reference tracer, but the calculated sensitivities can be directly converted to any other tracer by multiplication with the ratio of the corresponding molecular masses (m_{CH4} and m_X):

$$sensitivy\ tracer\ X \left[\frac{ppb\ X}{kg\ X\ s^{-1}}\right] = sensitivity\ CH4 \left[\frac{ppb\ CH4}{kg\ CH4\ s^{-1}}\right] \times \frac{m_{CH4}}{m_X}$$

The 3-monthly average sensitivities show a significant seasonal dependence, with larger sensitivities to emissions relatively close to the monitoring station during winter (most pronounced in the area ~50-100 km around the station; see also 'zoomed' presentation in Figure 5). This is probably largely due to the usually lower daytime boundary layer height in winter compared to summer. Furthermore, there is a significant diurnal variation of the sensitivity, especially in summer, with enhanced sensitivity ~50 km around the station during night, which is due to the shallow nocturnal boundary layer (Figure 6).

Figure 7 shows the 'radial surface sensitivity' [*Oney et al.*, 2015], describing the average sensitivity as function of distance from the measurement station. Following the approach of [*Oney et al.*, 2015] we evaluate also the radius τ_{s50} at which the cumulative surface sensitivity reaches 50% of the total sensitivity over the whole COSMO-7 model domain. The radius τ_{s50} can be seen as measure for the scale at which the measurements inform about the emissions. Since the 'radial surface sensitivity' is in general much higher during night than during day at distances up to 50-100 km around the station, especially during summer, the radius τ_{s50} is much smaller during night (~57 km in summer) than during day (~187 km in summer). The larger relative impact of the emissions closer to the station, reflected in the smaller τ_{s50} radius, makes it more difficult to disentangle the information about the emissions at larger distances.

Figure 7 also shows the benefit of the increase of sampling height, with the 100m sampling point being typically a factor 2 less sensitive to nearby emissions (~10 km). The increase of the τ_{s50} radius, however, is only relatively small (on the order of 20%). In reality, the benefit of increased sampling height is probably larger owing to the much lower sensitivity of the higher sampling point to local emissions close to the station which are not resolved by the model.

FLEXPART simulations driven by COSMO-2 meteorology have been found to be too diffusive compared to simulations driven by COSMO-7 or ECMWF meteorology. As a consequence, the footprints presented in this study likely drop off too quickly with distance from the site

as compared to reality. The area of sensitivity of the Ispra site presented here is thus likely a lower estimate.

In addition to the seasonal and diurnal variations, synoptic variability plays an important role. As an example, we show in Figures 8a and 8b the footprints on 19 January 2011. While the footprint between 0:00 and 6:00 is largely confined to the North-Western Po valley (and adjacent mountain area), around 9:00 a significant westerly flow develops, turning later on this day to Northwest / North, and advecting air from the Atlantic over Ireland and the UK to the monitoring station.

In the following, we analyse again the sensitivities as function of distance from the monitoring station, but now looking on the whole time series 2011, showing in detail the dynamic evolution due to the diurnal, synoptic and seasonal variability. For this purpose we define different sectors as function of distance from the monitoring station as shown in Figures 9a and 9b. Figure 10a shows the relative contribution of the different sectors to the total signal (i.e. the ratio of the footprint coming from the corresponding sector to the total footprint over the whole model domain) for the sampling height of 15m above surface (for the COSMO-2 based back trajectories). This analysis shows pronounced diurnals cycles especially between March and October, with a maximum contribution of the area up to 60 km around the station in the late night, while in the morning the relative influence of the areas further away increases significantly, usually reaching a maximum in the early afternoon. Typically the area at distances of more than 60 km contributes on the order of 50-80% of the total signal in the afternoon. The influence of this 'medium' to 'far-field' area, however, is on average smaller during winter, consistent with the smaller τ_{s50} radius discussed above (Figure 7). Nevertheless, the relative influence of the area beyond 60 km can reach also in winter occasionally a fraction of up to ~80% under synoptic conditions with high wind speeds.

Figure 10b shows the same analysis as Fig. 9a, but for the new sampling height of 100m above the surface. The comparisons of the two figures show the significant reduction of the influence of the local sector (at distances between 0 and 3 km from the station), typically by a factor of about 2-3. This again demonstrates the benefit of the increased sampling height, aiming at better overall representativeness of the measurements on larger regional scales.

In Figure 10c we show the same analysis, but for the whole COSMO-7 domain (merging the 2 inner sectors defined for COSMO-2 to a single 0-10 km sector, and adding an additional 'far-field' sector for distances larger than 1000 km). Overall, the COSMO-2 and COSMO-7 figures are largely consistent, but the analysis for the whole COSMO-7 domain shows usually a larger contribution from the 400-1000 km sector (which is only partially covered by the COSMO-2 domain. Furthermore, during particular synoptic events (with high wind speeds) the 'far-field' beyond 1000 km can contribute significantly.

Finally, we analyse the relative contribution of the sectors in different directions from the station (see Figure 11a and 11b for the definition of the different sectors). Figures 12a and 12b show the large synoptic variability including periods with dominant influence of each of the individual direction sectors (North, West, South, East). Furthermore, this analysis shows at many days a significant diurnal variability of the relative contributions of the different direction sectors, with a maximum of the northerly sector in the late night, and a maximum of the easterly and southerly sector in the afternoon. This diurnal pattern is most pronounced between April and October, and is apparently largely due to the diurnal variation in wind direction due to the regional mountain - lake/valley wind system discussed in section 3.

5. Conclusions and outlook

The sensitivity of the atmospheric signal at the monitoring station Ispra shows significant variations on diurnal, synoptic and seasonal scales. The atmospheric concentrations at the monitoring station have a strong sensitivity to emissions from the North-Western Po valley, but under specific synoptic situations also to areas at much larger distances. The sensitivity shows usually a significant diurnal cycle, during night dominated by the area 40-60 km around the station, while daytime footprints are much larger, typically dominated by the area at distances of more than 60 km. During summer daytime, the radius τ_{s50} (at which the cumulative surface sensitivity reaches 50% of the total sensitivity) is on average about 187 km. Our analysis shows that the future sampling at the Ispra tall tower 100m above ground significantly reduces the impact of local emissions (~3-10 km around the station) compared to the previously used sampling height of 15m above ground.
The diurnal cycle in local wind direction due to the regional mountain - lake/valley wind system leads to a significant diurnal cycle of the sensitivity (north-west vs. south-east), especially during summer time. This regional wind system implies that high-resolution atmospheric transport models (such as the FLEXPART / COSMO-2 systems used in this study) are required to properly interpret the atmospheric measurements. At the same time, the comparison between COSMO-2 and COSMO-7 demonstrates that also the 'far-fields' (at distances beyond 400 km / 1000 km; which are outside the COSMO-2 domain) play an important role. While atmospheric models currently used for flux inversions on the European scale (such as TM5-4VAR with a (zoom) resolution of 1^{o}(longitude) x 1^{o}(latitude), i.e. ~100 km) do not resolve the small scales (and the regional wind systems observed at the Ispra site), a promising approach is the coupling of high-resolution regional models (such as COSMO-2) with models of medium resolution (such as TM5-4VAR) for the wider European (and global) domain.

6. Acknowledgments

We thank Sebastiao Martins Dos Santos and Carsten Grüning for providing the meteo data from the JRC EMEP station. Furthermore, we are grateful to Alessandro Cescatti for discussions of this study.

7. References

Bergamaschi, P., et al. (2015), Top-down estimates of European CH_4 and N_2O emissions based on four different inverse models, *Atmos. Chem. Phys.*, *15*, 715-736.

Oney, B., D. Brunner, S. Henne, M. Leuenberger, I. Bamberger, I. Eugster, and N. Gruber (2015), The CarboCount CH sites: characterization of a dense greenhouse gas observation network, *manuscript in preparation*.

Putaud, J. P., et al. (2014), JRC – Ispra Atmosphere – Biosphere – Climate Integrated monitoring Station 2013 report, *Report EUR 26995 EN*, European Commission Joint Research Centre Institute for Environment and Sustainability.

Scheeren, H. A., and P. Bergamaschi (2012), First Three Years of CO_2, CH_4, N_2O, and SF_6 Observations, and ^{222}Radon-Based Emission Estimates from the JRC Monitoring Station

at Ispra (Italy): What Have We Learned So Far? , proceedings of the 16th WMO/IAEA Meeting on Carbon Dioxide, Other Greenhouse Gases and Related Measurement Techniques (GGMT-2011), Wellington, New Zealand, World Meteorological Organization.

Schraff, C. H. (1997), Mesoscale data assimilation and prediction of low stratus in the Alpine region, , *Meteorology and Atmospheric Physics*, *64*, 21–50.

Stohl, A., C. Forster, A. Frank, P. Seibert, and G. Wotawa (2005), Technical note: The Lagrangian particle dispersion model FLEXPART version 6.2, *Atmos. Chem. Phys.*, *5*, 2461–2474.

Tiedtke, M. (1987), A comprehensive mass flux scheme for cumulus parameterization in large-scale models, *Monthly Weather Review*, *117*, 1779-1800.

8. Figures

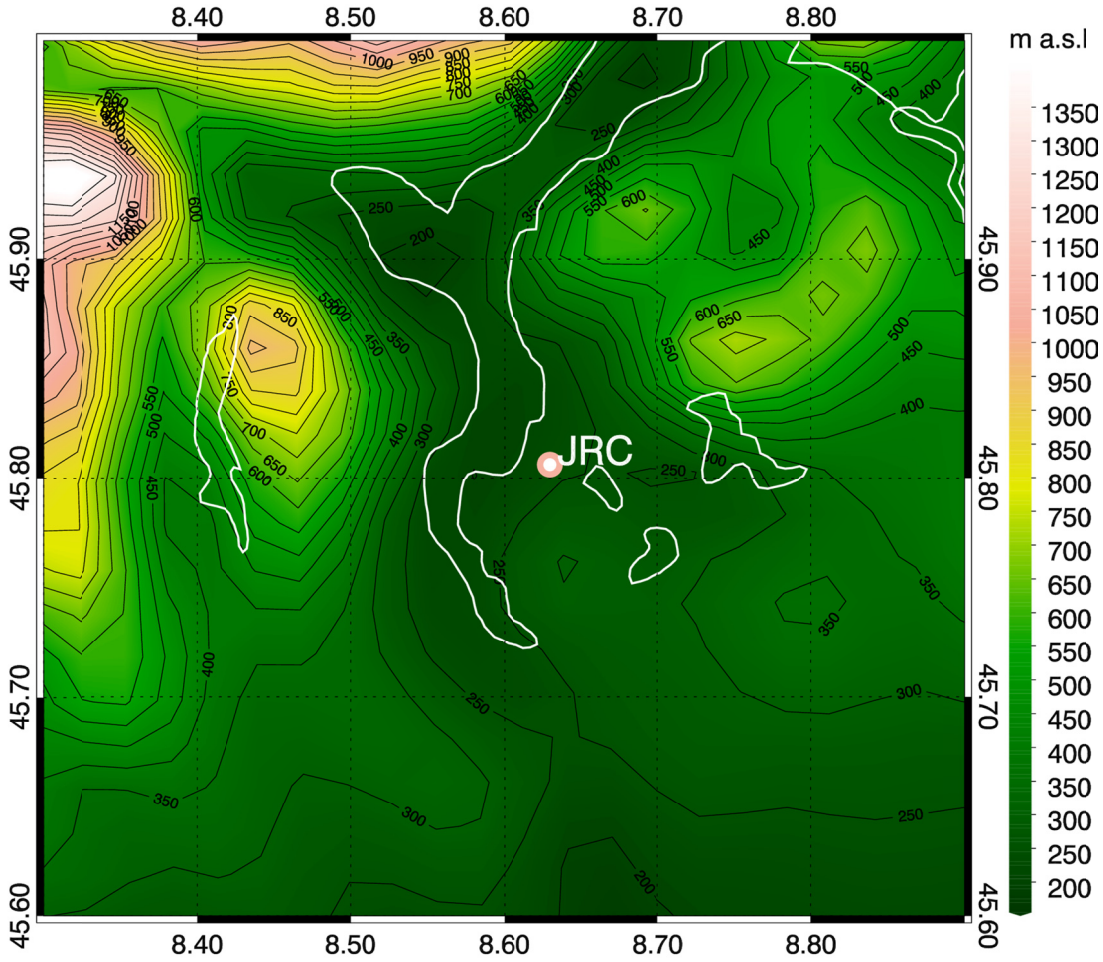

Figure 1: Topography of COSMO-2 model around the JRC Ispra Atmosphere - Biosphere - Climate Integrated monitoring Station (ABC-IS).

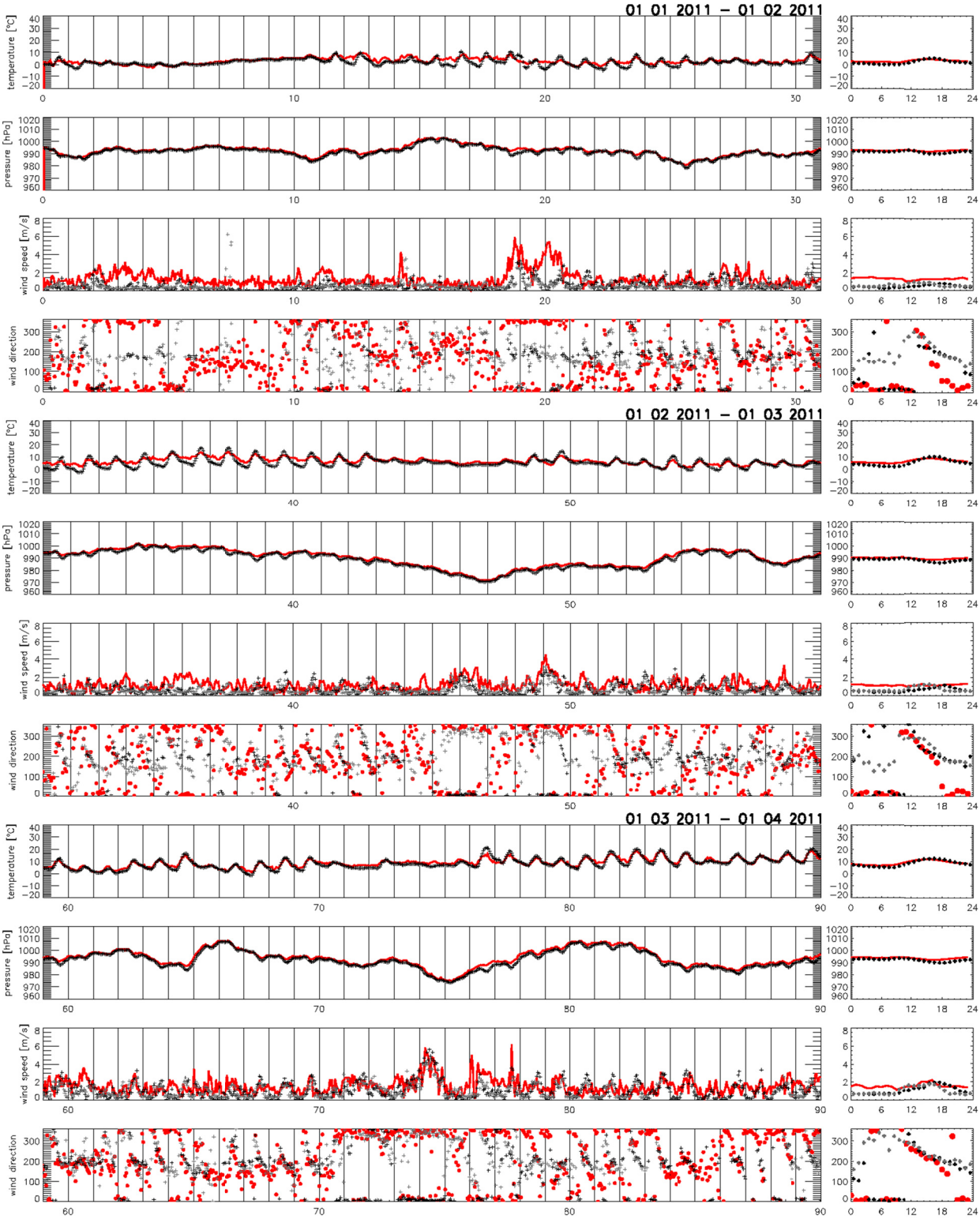

Figure 2a: Simulated and observed meteorological parameters for period 01 January 2011 until 01 April 2011. Rows show monthly time series of temperature, pressure, wind speed, and wind direction. Red curves (and red symbols) are simulated values from COSMO-2, black symbols observations at the JRC ARPA meteo station, and grey symbols observations at the JRC EMEP meteo station (for wind speed and wind direction only). Observed wind direction is plotted only for wind speeds above 0.5 m/s. Black vertical lines indicate the 0:00 time of each day. The small panels on the right side show mean diurnal cycles (averaged over the corresponding month).

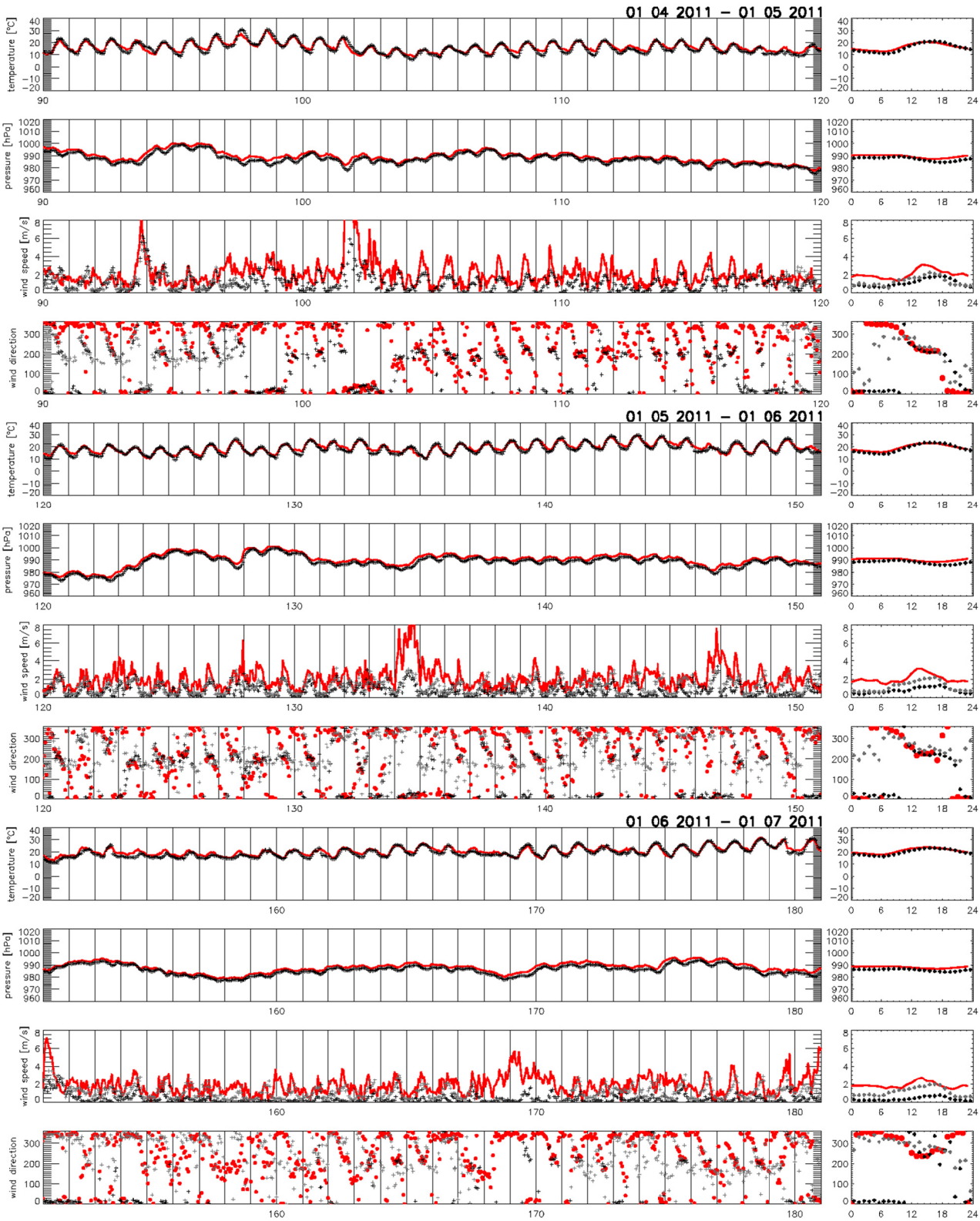

Figure 2b: Same as Fig. 2a, but for 01 April until 01 July 2011.

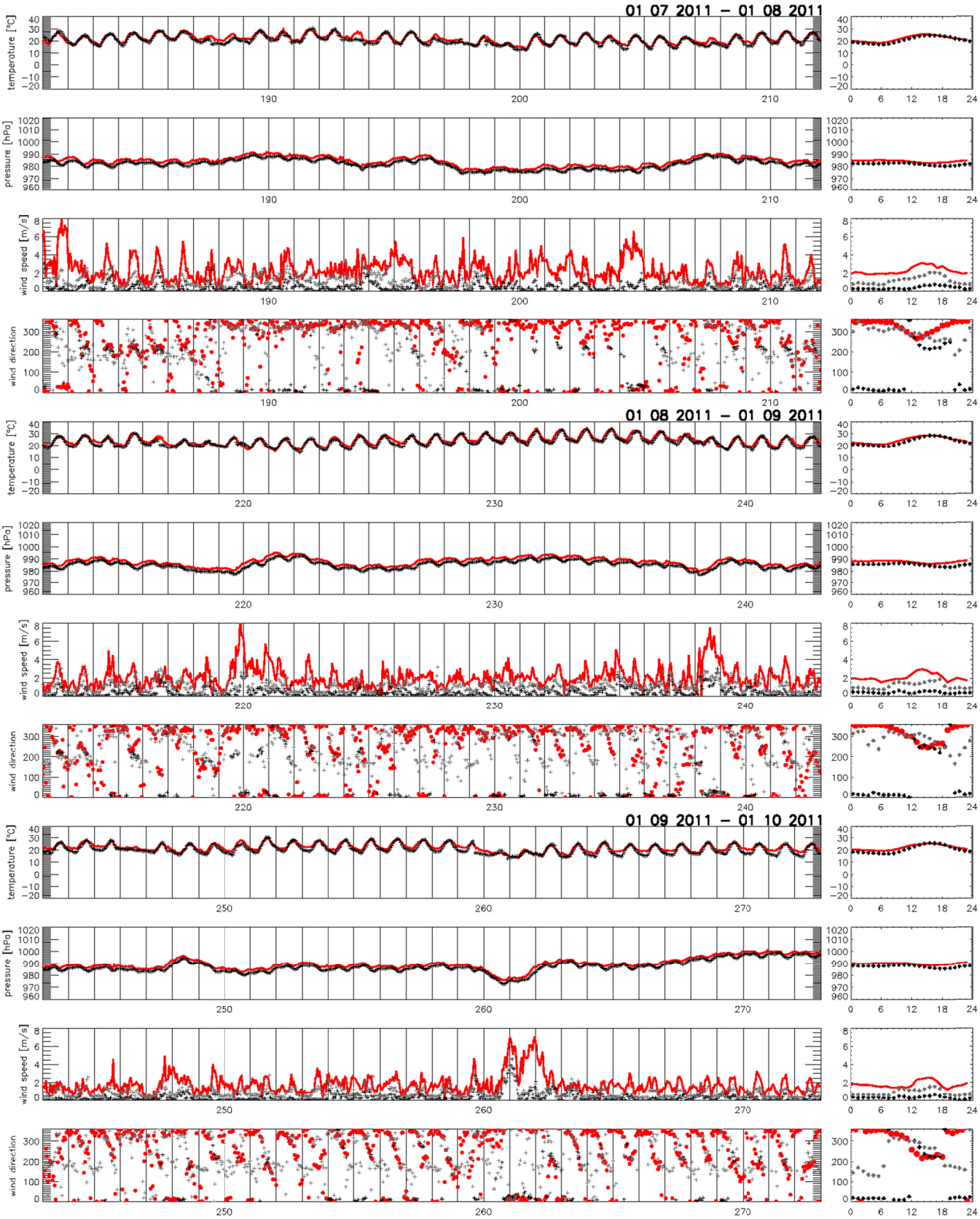

Figure 2c: Same as Fig. 2a, but for 01 July until 01 October 2011.

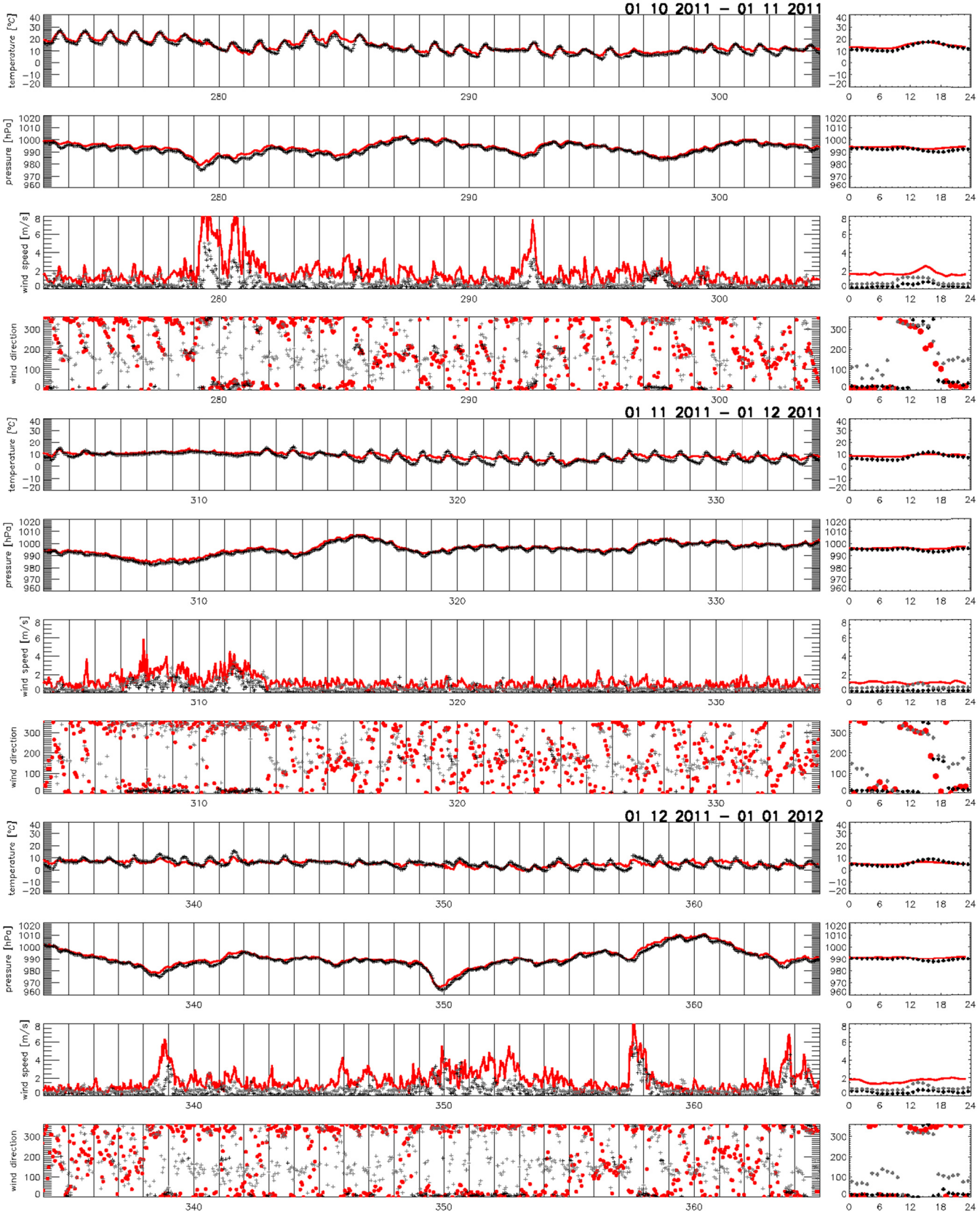

Figure 2d: Same as Fig. 2a, but for 01 October 2011 until 01 January 2012.

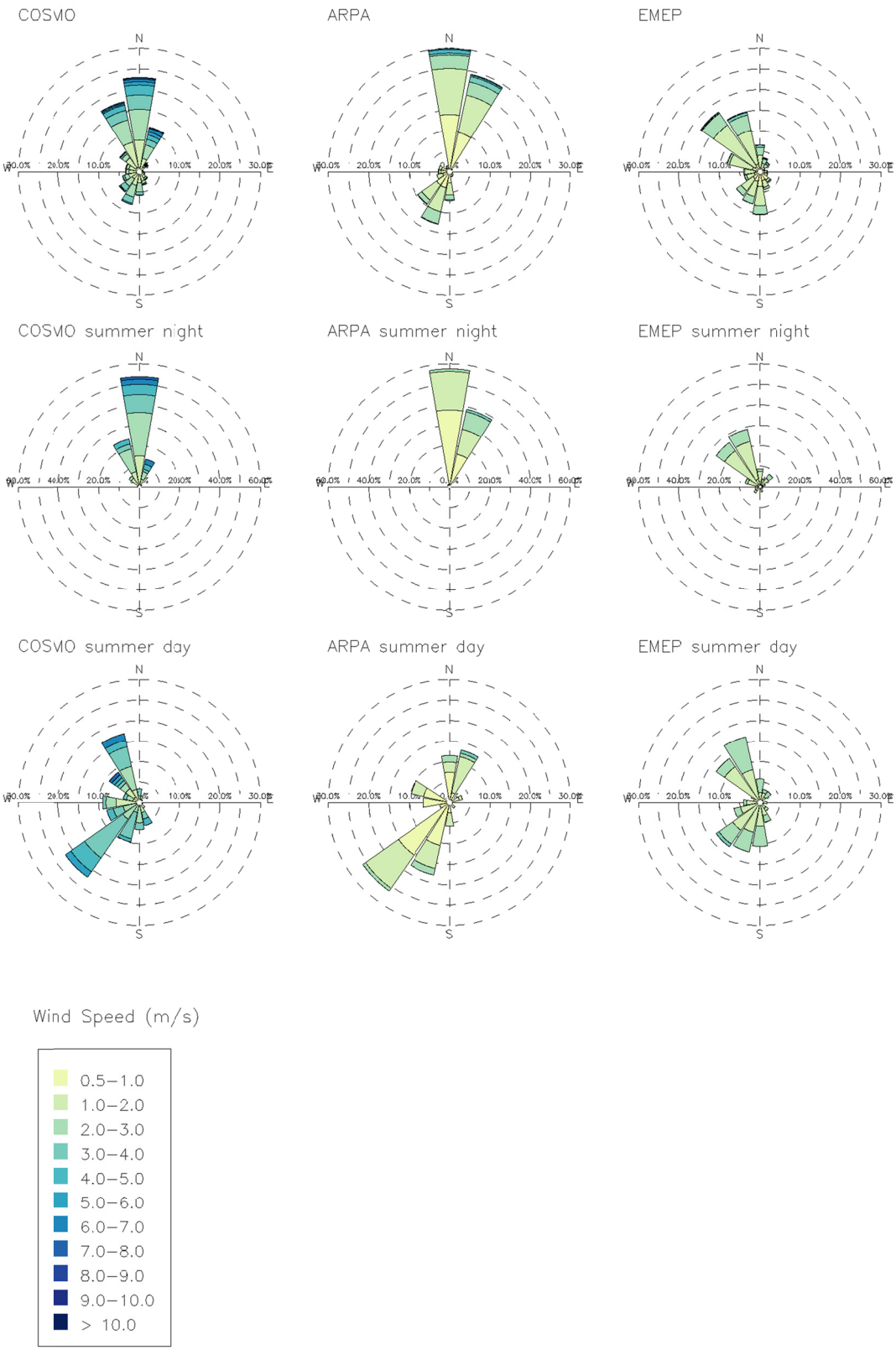

Figure 3: Frequency Distribution of wind direction and wind speed ('wind roses'). Left: COSMO-2; middle: measurements at ARPA meteo station; right: measurements at EMEP meteo station. Upper panel: whole year; middle panel: summer (JJA) nighttime; lower panel: summer daytime. In all cases model and meteo data were extracted consistently (i.e. hourly data only used, if data from both meteo stations are available, and if wind speed is above threshold of 0.5 m/s for all three data sets)

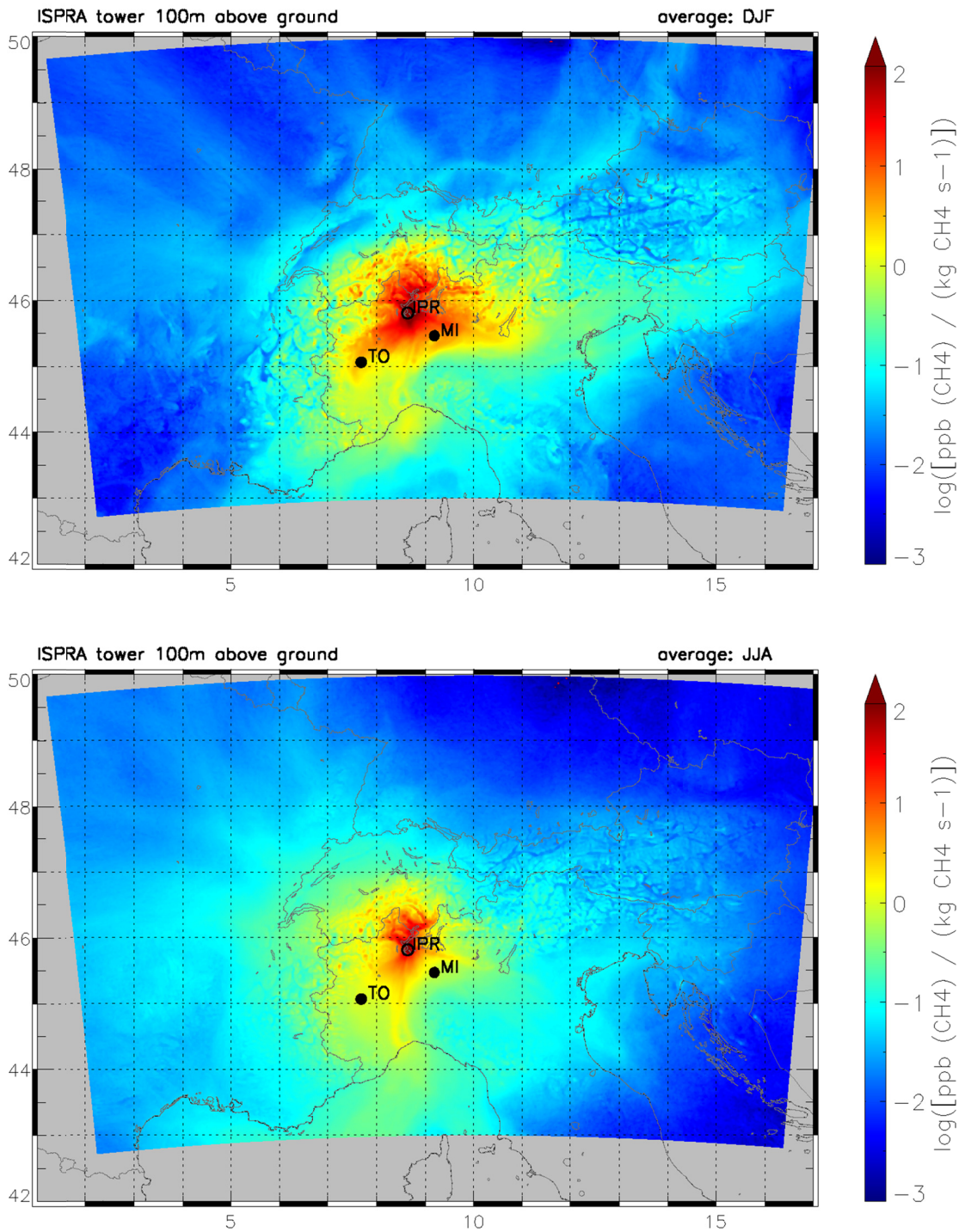

Figure 4a: Seasonal average sensitivities of atmospheric concentration measurements at Ispra (IPR) to emissions ('footprints'), based on COSMO-2: Whole COSMO-2 domain. 'MI' and 'TO' indicate the cities of Milano and Torino, respectively. Top: winter; bottom: summer.

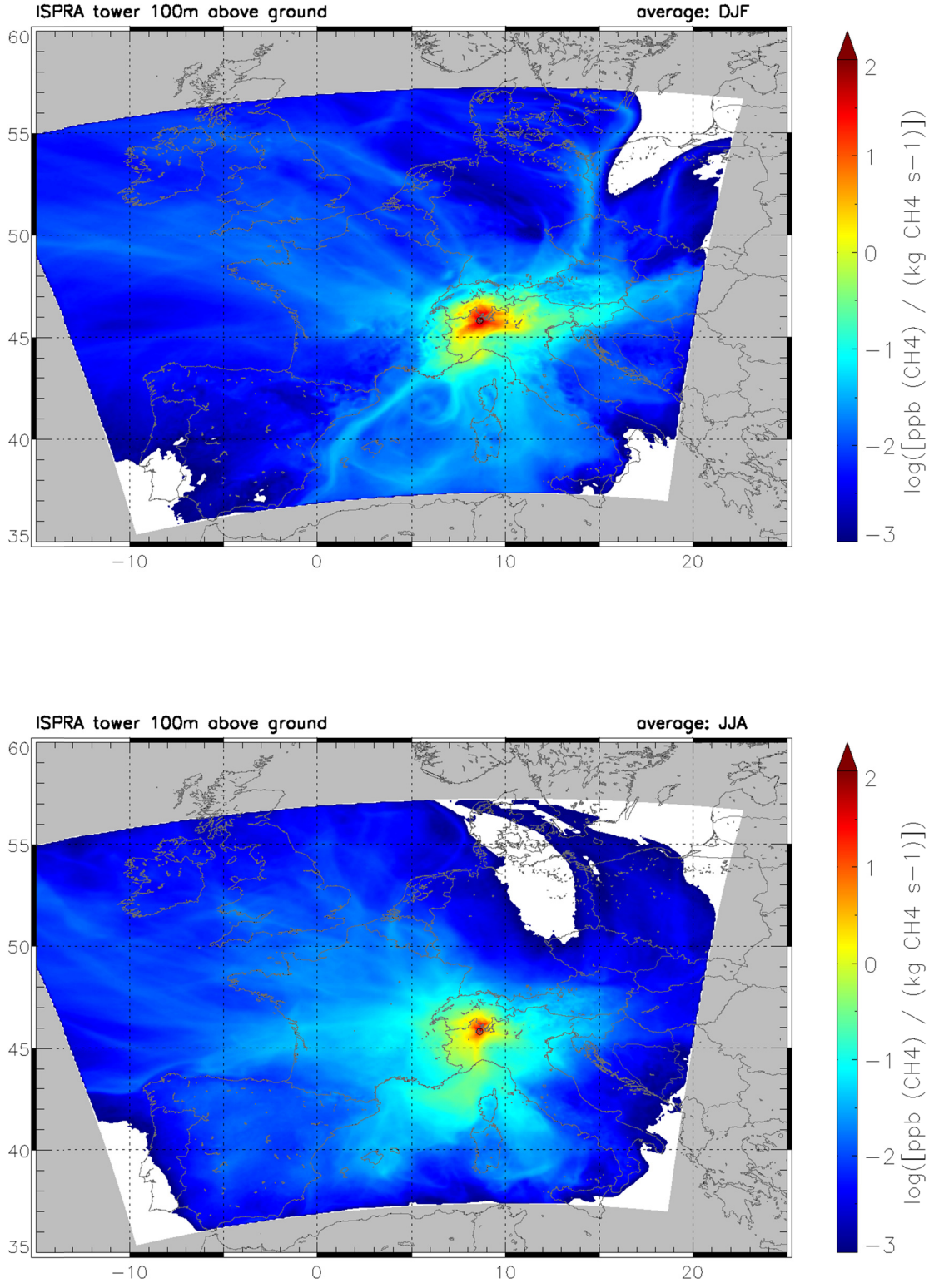

Figure 4b: Seasonal average sensitivities of atmospheric concentration measurements at Ispra (IPR) to emissions ('footprints'), on whole COSMO-7 domain. Top: winter; bottom: summer.

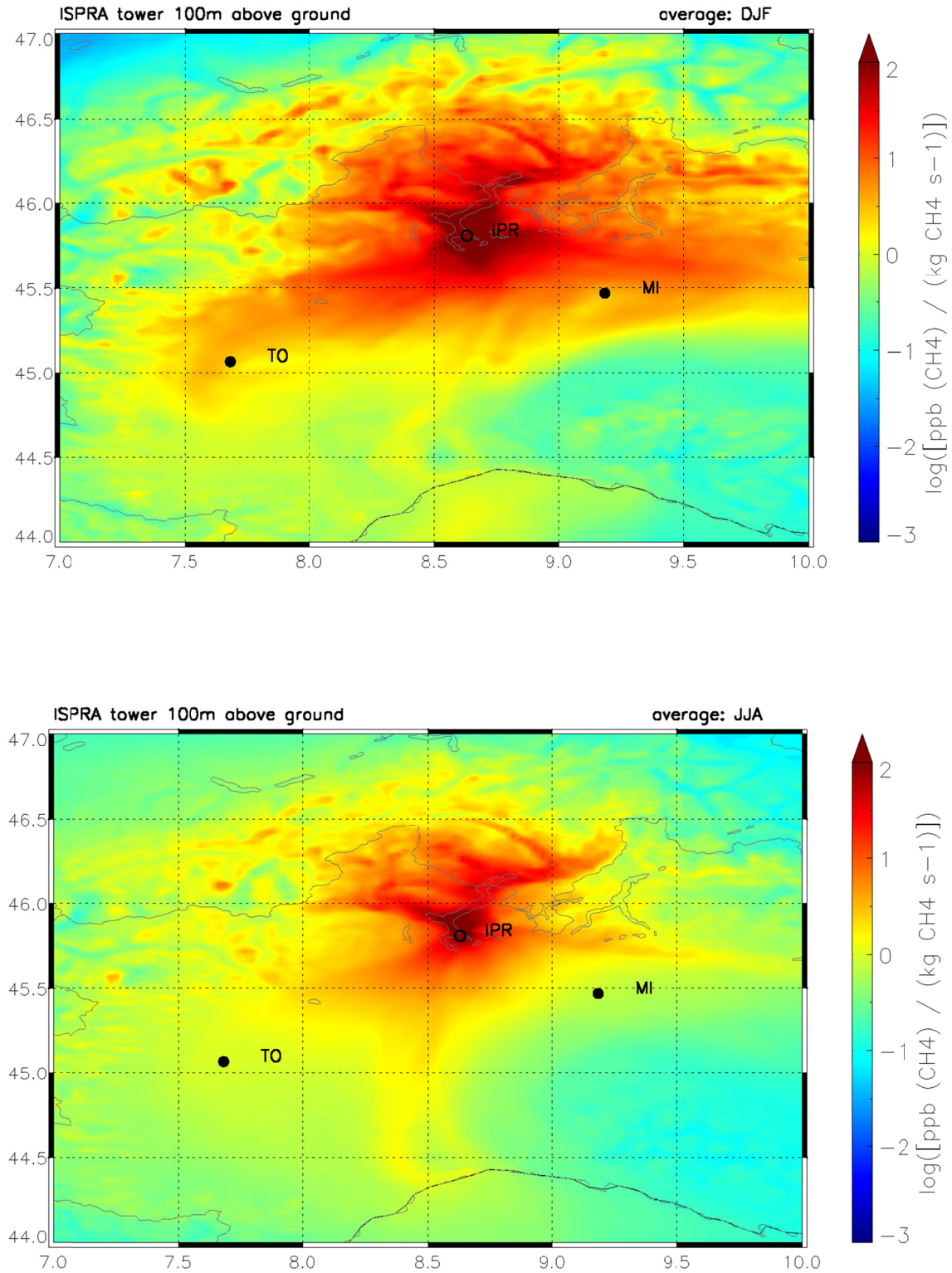

Figure 5: Seasonal average sensitivities of atmospheric concentration measurements at Ispra (IPR) to emissions ('footprints'), based on COSMO-2. Same as Figure 4a, but zoomed in over the inner part of the COSMO-2 around IPR. Top: winter; bottom: summer.

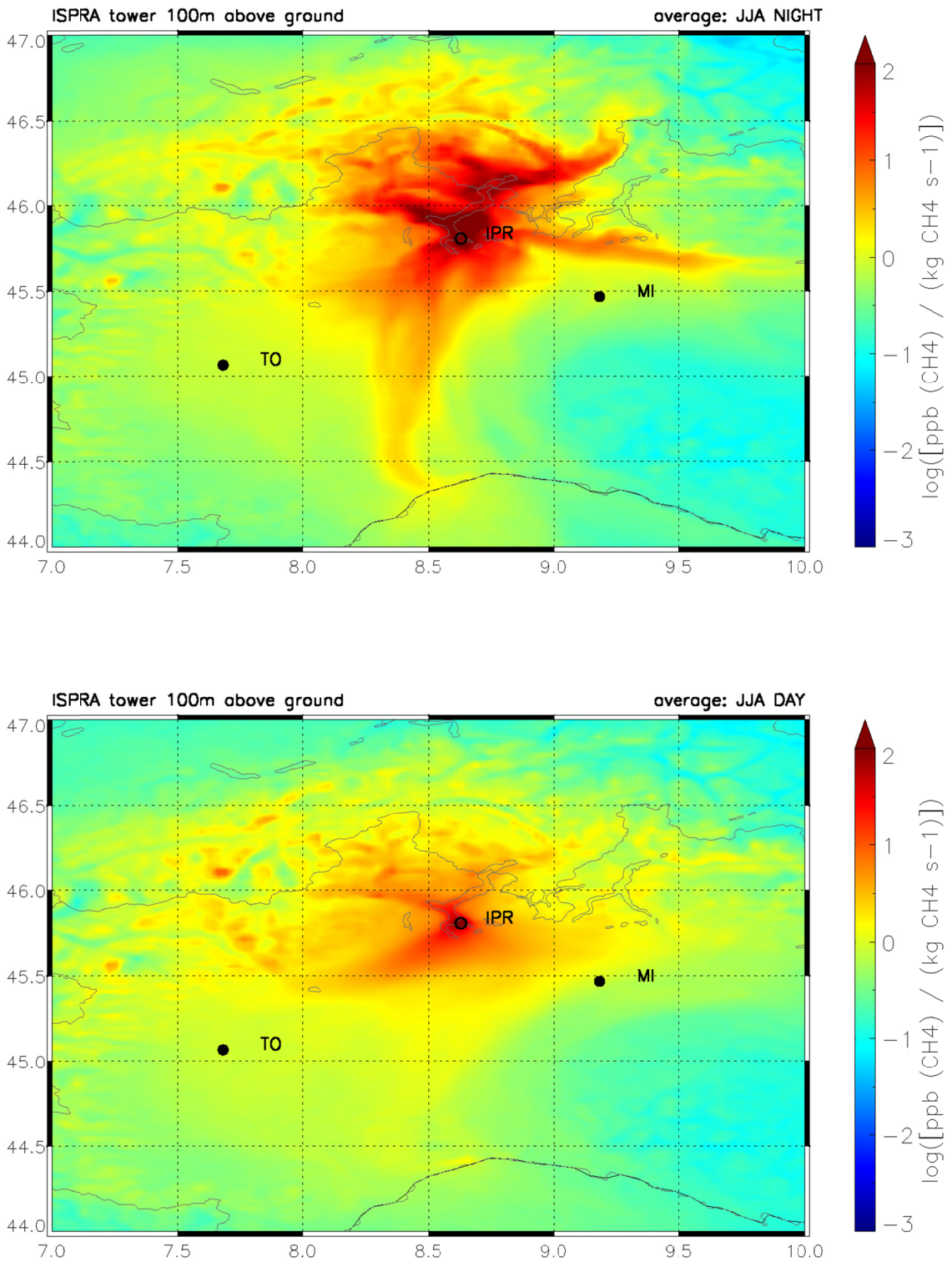

Figure 6: Impact of daytime on sensitivity in summer (JJA): Top: average sensitivity during night; bottom: average sensitivity during day.

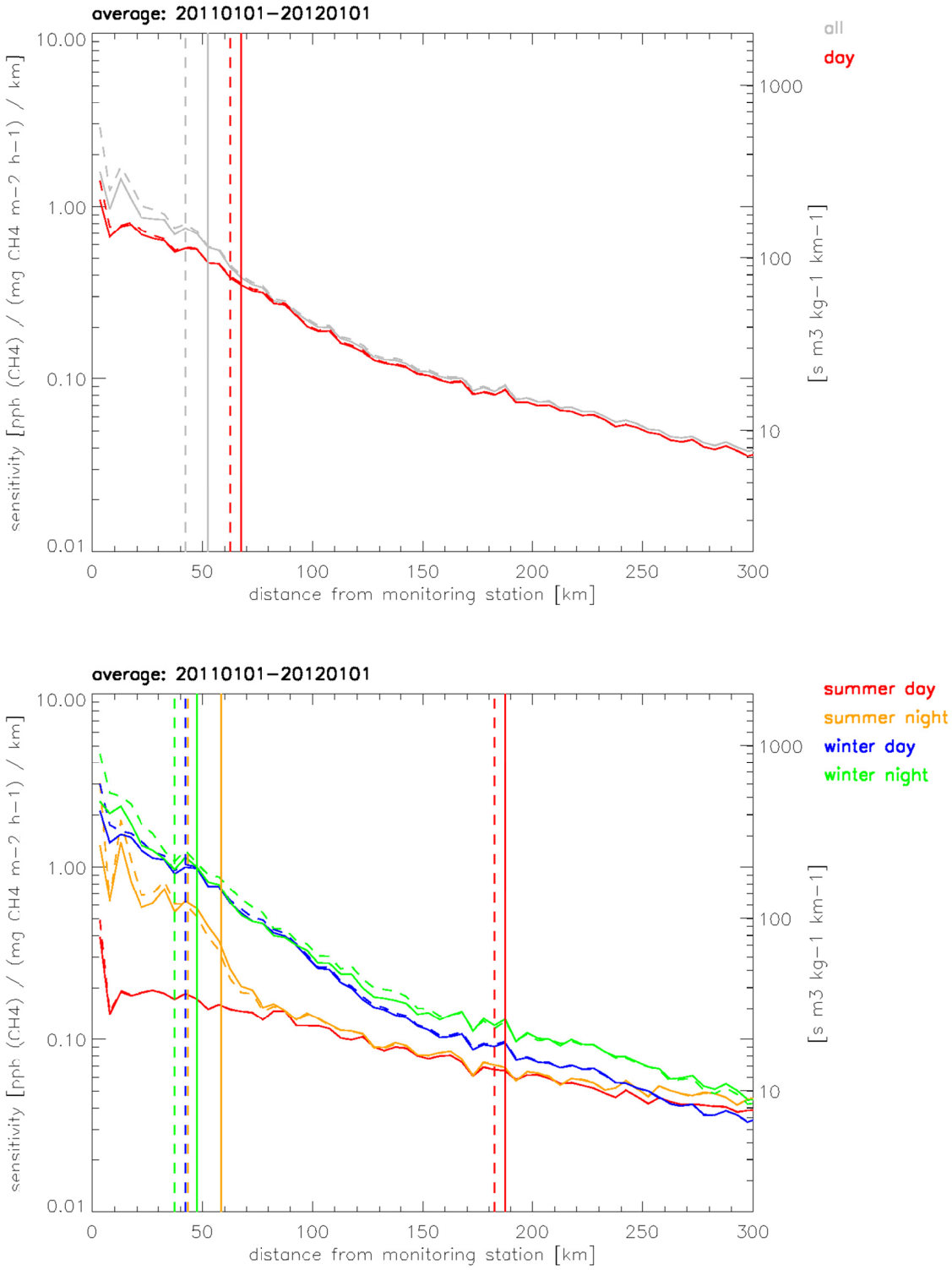

Figure 7: Sensitivity as function of distance from monitoring station IPR ("Radial surface sensitivity"). Top: Annual average sensitivity. Grey: average over whole diurnal cycle. Red: Daytime measurements only. Solid line: 100m sampling point; Dashed line: 15m sampling point. The vertical lines indicate the radius where the integrated sensitivity reaches 50% of total sensitivity over whole COSMO-7 domain. Bottom: Radial surface sensitivity during day and during night, for summer and for winter.

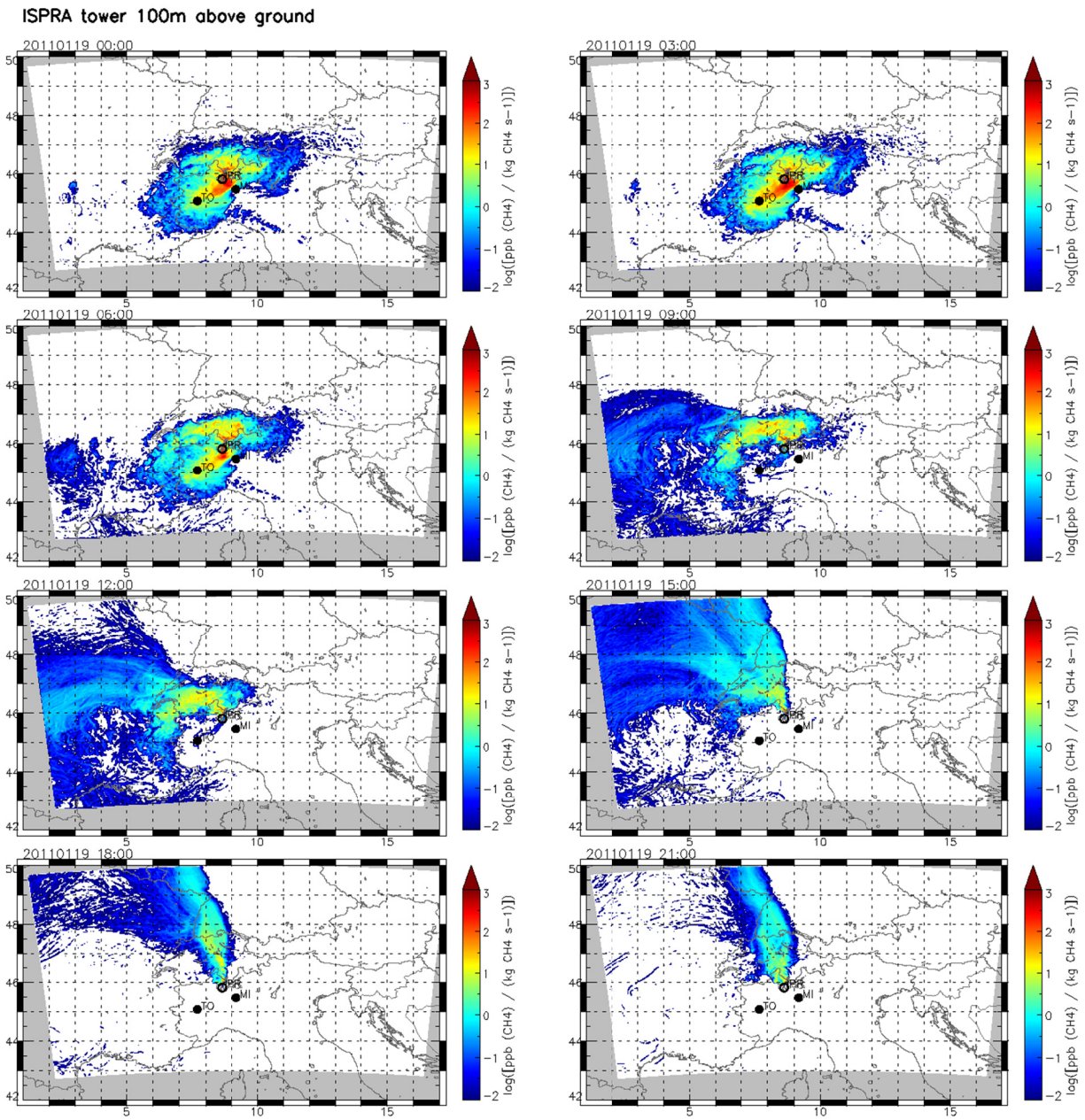

Figure 8a: Synoptic variability: Evolution of total footprints (COSMO-2) on 19 January 2011.

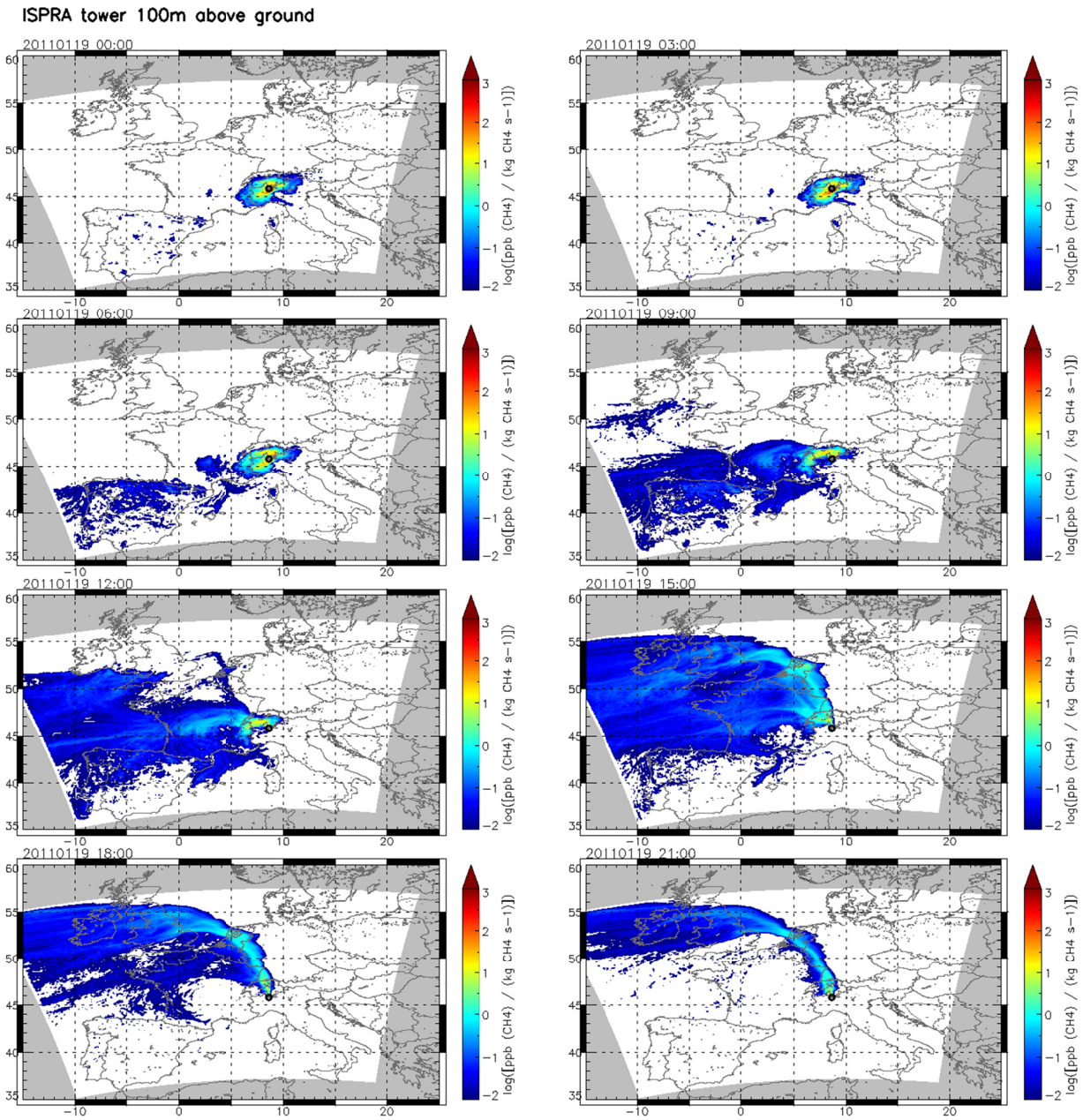

Figure 8b: Synoptic variability: Evolution of total footprints (COSMO-7) on 19 January 2011.

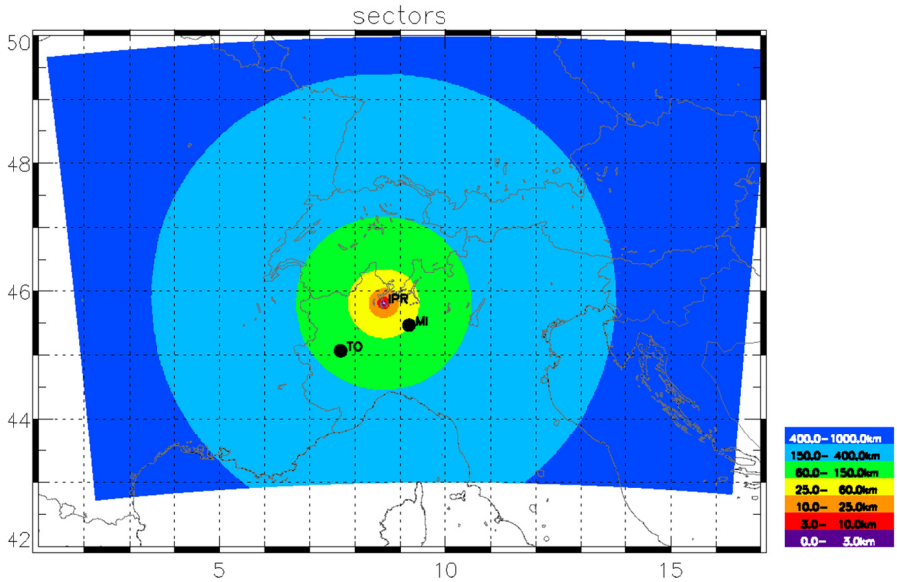

Figure 9a: Definition of different sectors (based on distance from monitoring station Ispra; COSMO-2) used for analysis shown in Fig. 10a and 10b.

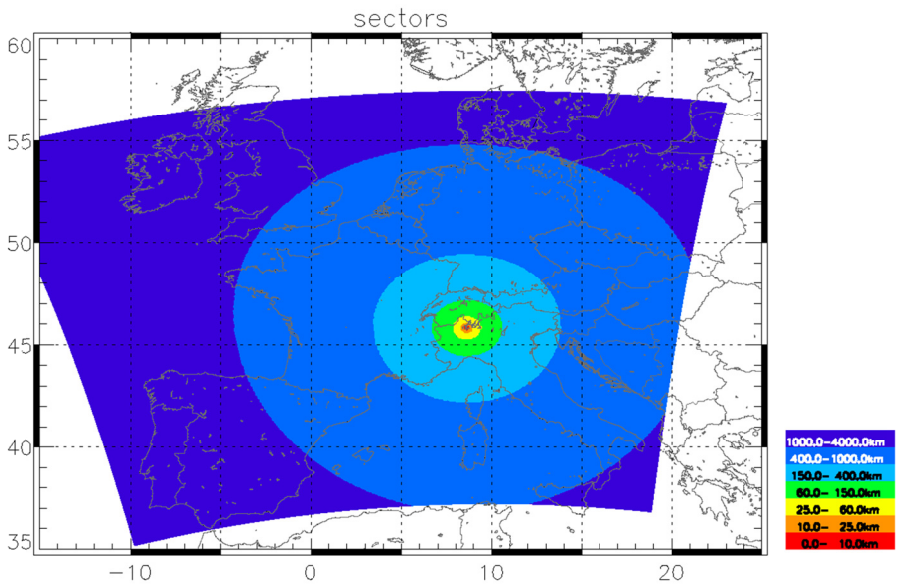

Figure 9b: Definition of different sectors (based on distance from monitoring station Ispra; COSMO-7) used for analysis shown in Fig. 10c.

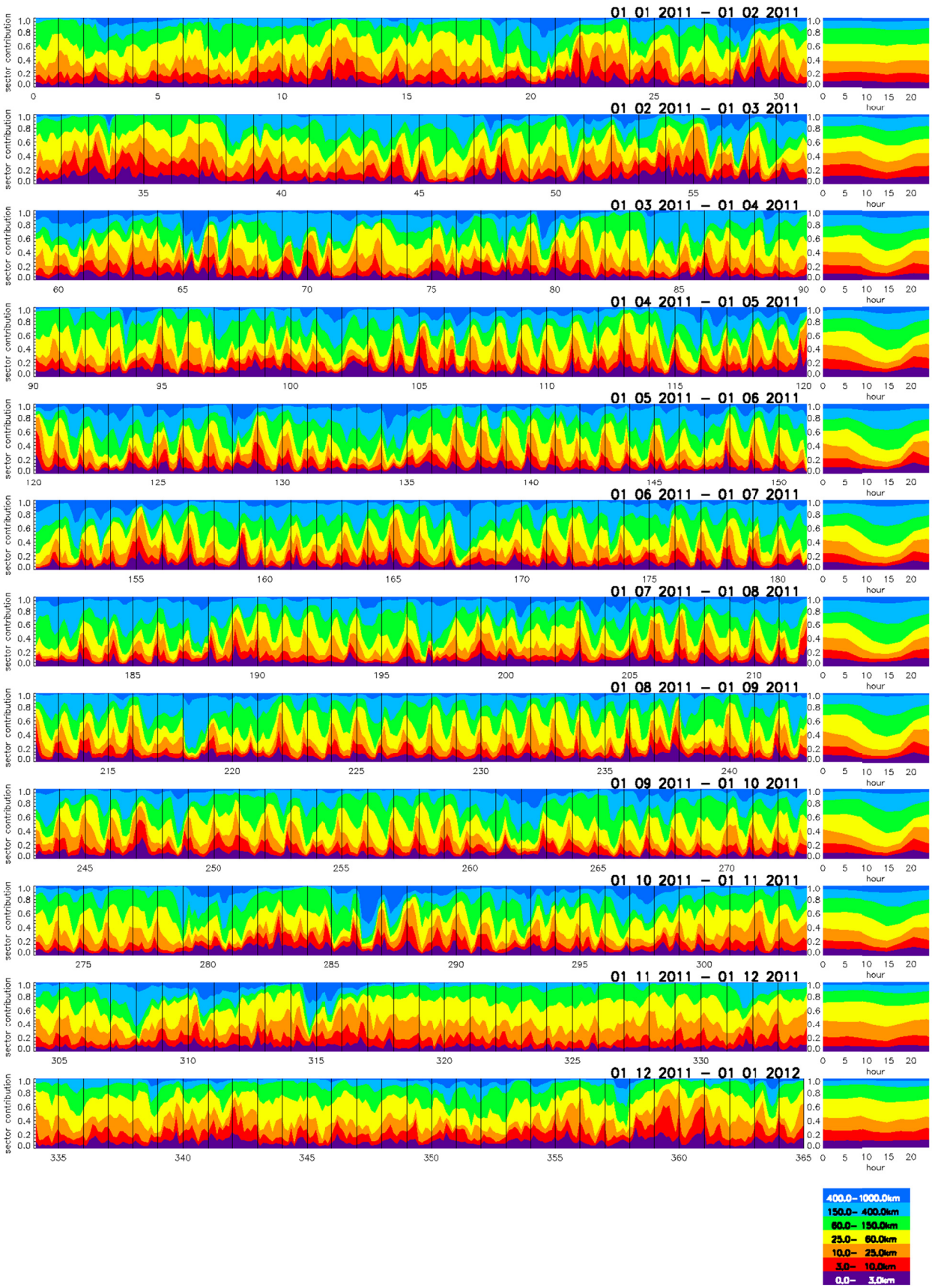

Figure 10a: Relative contribution of different sectors (defined by distance from monitoring station Ispra, see Fig. 9a) to total signal (within COSMO-2 domain) for sampling height of 15m above surface.

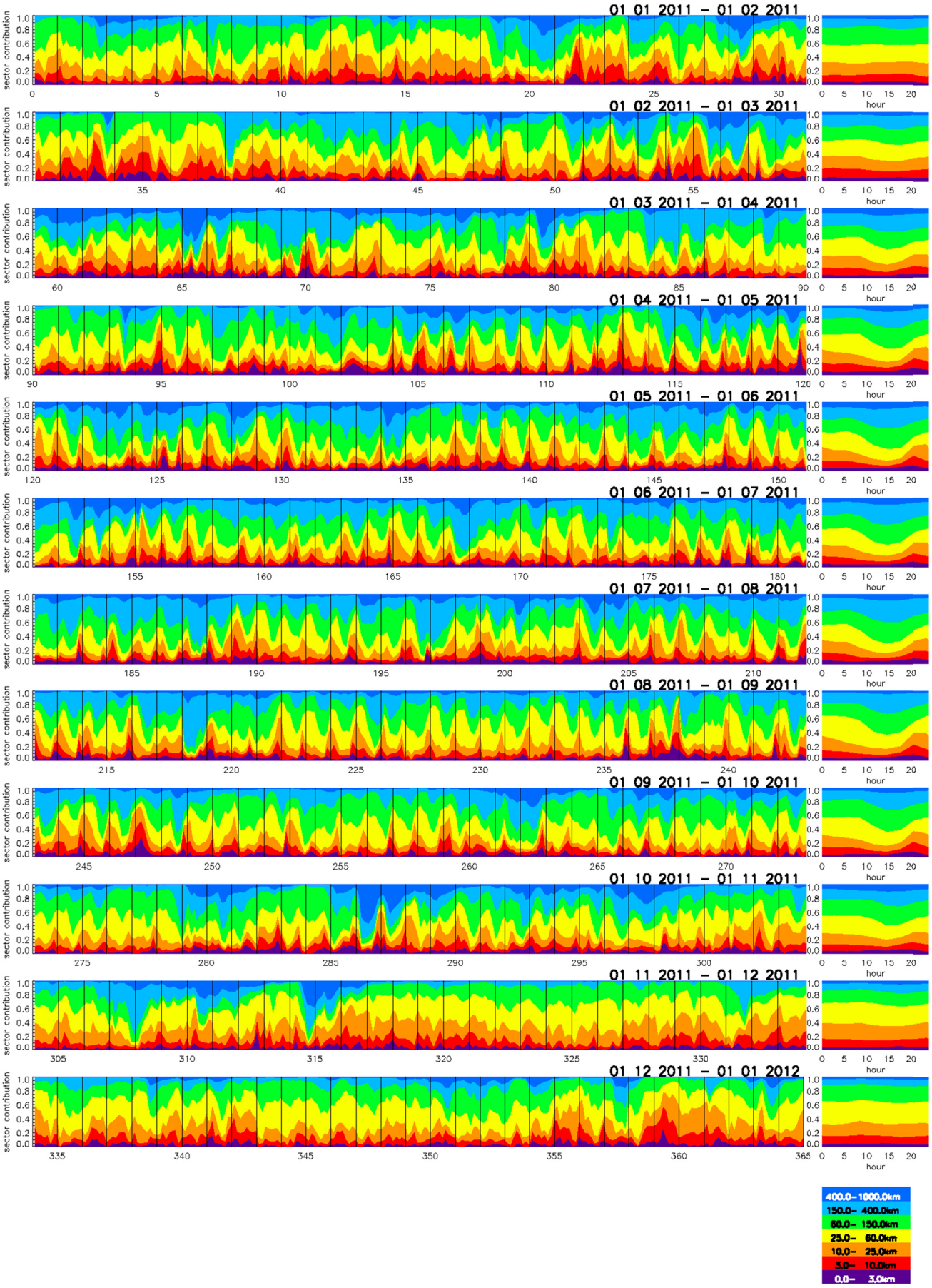

Figure 10b: Same as Fig. 10a, but for sampling height of 100m above surface.

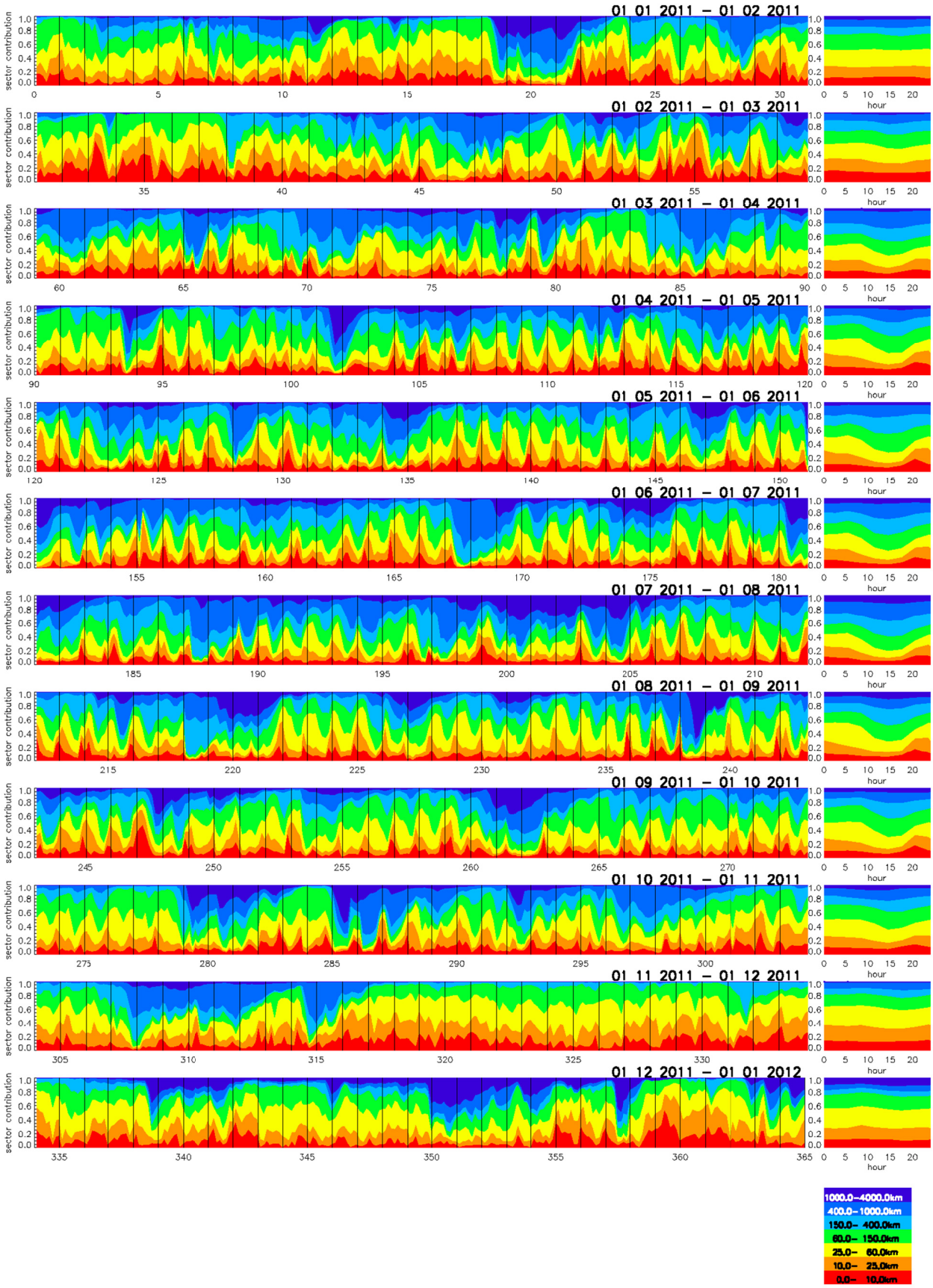

Figure 10c: Relative contribution of different sectors (defined by distance from monitoring station Ispra, see Fig. 9b) to total signal (within COSMO-7 domain) for sampling height of 100m above surface.

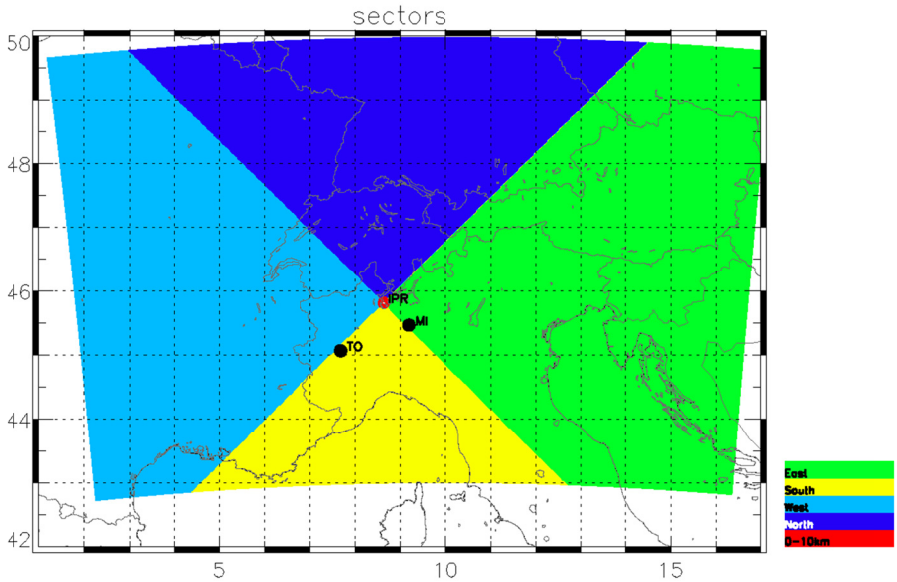

Figure 11a: Definition of different sectors (based on direction from monitoring station Ispra; COSMO-2) used for analysis shown in Fig. 12a.

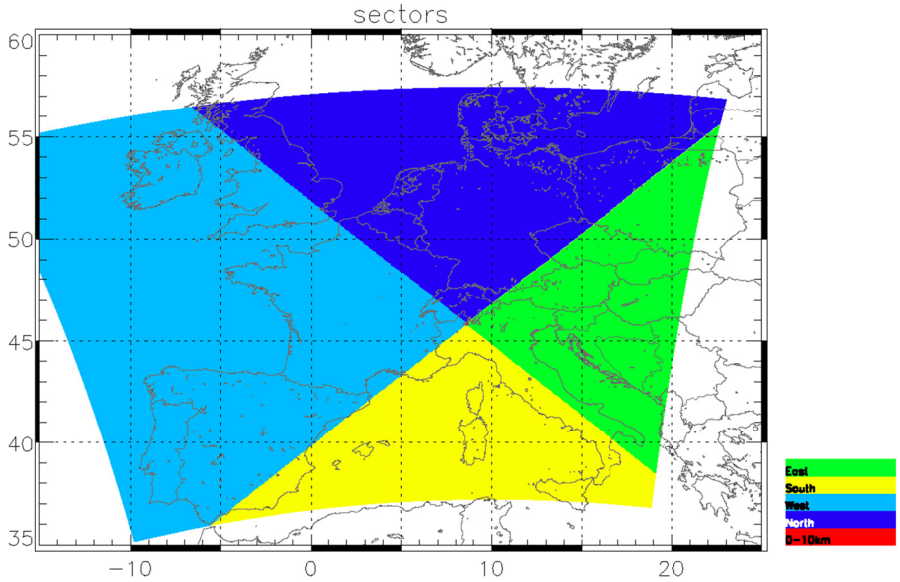

Figure 11b: Definition of different sectors (based on direction from monitoring station Ispra; COSMO-7) used for analysis shown in Fig. 12b.

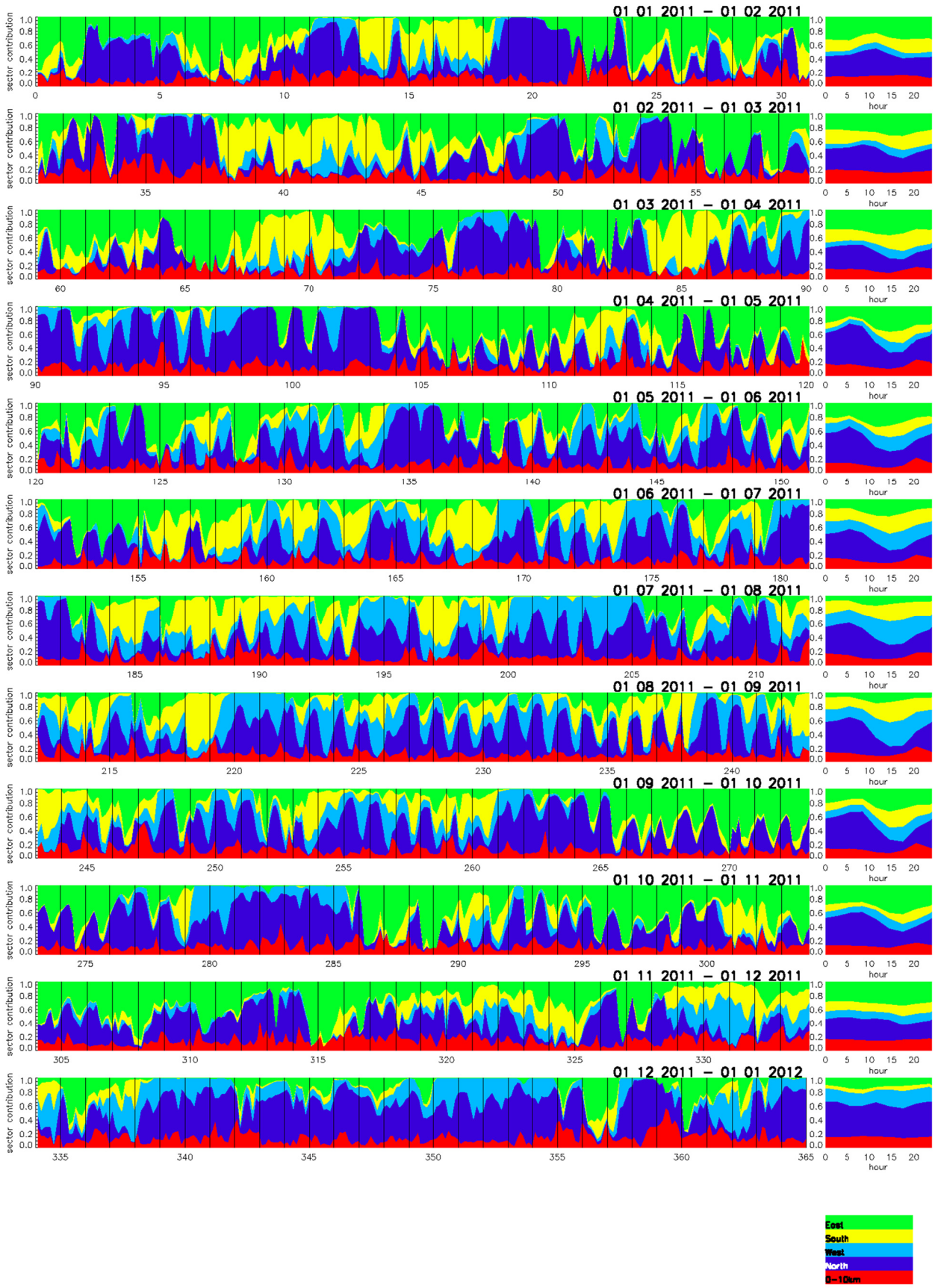

Figure 12a: Relative contribution of different sectors (defined by direction from monitoring station Ispra, see Fig. 11a) to total signal (within COSMO-2 domain) for sampling height of 100m above surface.

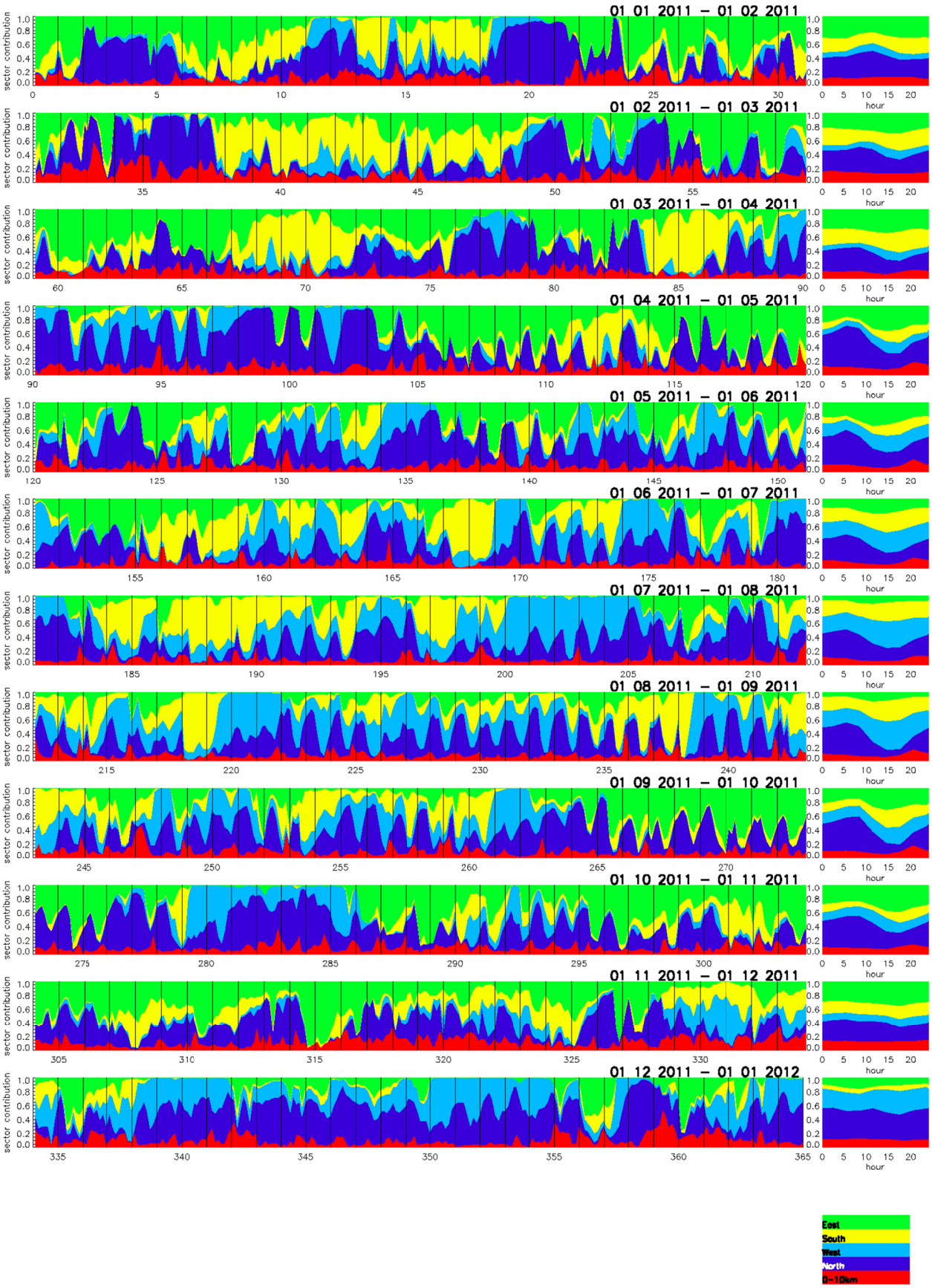

Figure 12b: Relative contribution of different sectors (defined by direction from monitoring station Ispra, see Fig. 11b) to total signal (within COSMO-7 domain) for sampling height of 100m above surface.

European Commission
EUR 27131 EN– Joint Research Centre –Institute for Environment and Sustainability

Title: Analysis of the sensitivity of atmospheric measurements at the JRC Ispra Atmosphere - Biosphere - Climate Integrated monitoring Station

Author(s): Peter Bergamaschi and Dominik Brunner

Luxembourg: Publications Office of the European Union

2015 – 32 pp. – 21.0 x 29.7 cm

EUR – Scientific and Technical Research series – ISSN 1831-9424 (online)

ISBN 978-92-79-46164-4 (PDF)

doi: 10.2788/234440

LB-NA-27131-EN-N

JRC Mission

As the Commission's in-house science service, the Joint Research Centre's mission is to provide EU policies with independent, evidence-based scientific and technical support throughout the whole policy cycle.

Working in close cooperation with policy Directorates-General, the JRC addresses key societal challenges while stimulating innovation through developing new methods, tools and standards, and sharing its know-how with the Member States, the scientific community and international partners.

Serving society
Stimulating innovation
Supporting legislation

doi: 10.2788/234440

ISBN 978-92-79-46164-4

Publications Office